High-Accuracy Measurement of the Differential Scalar Polarizability of a $^{88}Sr^+$ Clock Using the Time-Dilation Effect

Pierre Dubé,* Alan A. Madej, Maria Tibbo, and John E. Bernard
Frequency and Time Group, Measurement Science and Standards Portfolio, National Research Council of Canada, Ottawa, Canada K1A 0R6

(Received 27 February 2014; published 29 April 2014)

We report a high-accuracy measurement of the differential static scalar polarizability $\Delta\alpha_0$ of the $5s\,^2S_{1/2} - 4d\,^2D_{5/2}$ transition of the $^{88}Sr^+$ ion. The high accuracy is obtained by comparing the micromotion-induced positive scalar Stark shift to the negative time-dilation shift. Measurement of the trap drive frequency where these shifts cancel is used to determine $\Delta\alpha_0$ without the need to determine the electric field. $\Delta\alpha_0$ is a critical parameter for the operation of frequency standards as it determines the blackbody radiation frequency shift coefficient, the largest source of uncertainty in the $^{88}Sr^+$ ion clock. The measured value of $\Delta\alpha_0$ is $-4.7938(71) \times 10^{-40}$ J m^2/V^2. Taking into account the dynamic correction, the blackbody shift at 300 K is 0.247 99(37) Hz. The contribution of the blackbody shift coefficient to the uncertainty of the ion standard has been reduced by a factor of 24, from 2×10^{-17} to 8.3×10^{-19}. The revised total uncertainty of our reference standard is 1.2×10^{-17}, limited by the blackbody field evaluation. An additional benefit of the low uncertainty of $\Delta\alpha_0$ is the ability to suppress, by a factor of about 200, the net micromotion frequency shifts.

DOI: 10.1103/PhysRevLett.112.173002 PACS numbers: 32.10.Dk, 06.30.Ft, 32.60.+i, 37.10.Ty

Optical atomic clocks have made phenomenal advances during the past 15 years, with several systems [1–8] surpassing by at least 1 order of magnitude the stability and precision of state-of-the-art cesium fountain clocks that currently define the SI second [9]. Optical clocks offer new possibilities for advancing applied and fundamental science, such as timekeeping, GPS navigation, geodesy, space exploration, and tests of fundamental physics [10–13]. Present-day performances of optical clocks combined with their fast-paced improvements make a strong case in favor of an eventual redefinition of the second with an optical standard [7,14,15].

The lowest fractional frequency uncertainties reported to date are 8.6×10^{-18} for an $^{27}Al^+$ ion clock [1], and recently 6.4×10^{-18} for a ^{87}Sr optical lattice clock [8]. Except for the $^{27}Al^+$ ion, and other group III ion candidates that benefit from a very small blackbody radiation (BBR) shift coefficient [16], most other ion and neutral atom clock transitions are currently limited in accuracy by the uncertainty of the BBR shift [8,17–19].

The frequency shift in Hz, $\Delta\nu_{BBR}$, caused by the interaction of the clock transition with the BBR field $\langle E^2\rangle_T$ is given by [20,21]

$$\Delta\nu_{BBR} = -\frac{1}{2h}\langle E^2\rangle_T \Delta\alpha_0(1+\eta), \quad (1)$$

where $\langle E^2\rangle_T = 8\pi^5(k_BT)^4/[15\epsilon_0(hc)^3]$. Here k_B is Boltzmann's constant, T the BBR field temperature, ϵ_0 the vacuum permittivity, h Planck's constant, and c the speed of light. For $T = 300$ K, $\langle E^2\rangle_T \simeq (831.943\ \mathrm{V/m})^2$. $\Delta\alpha_0 = \alpha_0(e) - \alpha_0(g)$ is the differential static scalar polarizability of the clock transition. e and g refer to the excited and ground states, respectively. η is a temperature-dependent dynamic correction to $\Delta\alpha_0$ that accounts for the response of the atomic levels to the BBR spectrum.

We recently reported a fractional frequency uncertainty of 2.3×10^{-17} for the $5s\,^2S_{1/2} - 4d\,^2D_{5/2}$ transition of $^{88}Sr^+$ [5,17]. Despite state-of-the-art atomic structure calculations [22], the value of $\Delta\alpha_0$, with a fractional uncertainty contribution of 2×10^{-17}, remains the main contributor to the uncertainty budget of $^{88}Sr^+$ [17]. The only viable approach at present to reduce this uncertainty is to make a high-accuracy experimental measurement of $\Delta\alpha_0$. For $^{88}Sr^+$, $\eta(300\ \mathrm{K}) = -0.009\,51(15)$ is both small and accurately known from the atomic structure calculations [21,22]. It contributes a fractional uncertainty of 8.4×10^{-20}. Consequently, only the static part of the differential polarizability $\Delta\alpha_0$ requires experimental investigation to reach levels of $\lesssim 10^{-18}$ on the BBR shift coefficient evaluation for a known value of T.

Experiments to measure $\Delta\alpha_0$ were recently conducted for Yb [18] and Sr [19] neutral atom clock systems. The approach used was to measure the frequency shift of the clock transition caused by applying dc electric fields using precision parallel-plate capacitors. This type of measurement is not adapted to ions located in trapping fields.

Measurement of $\Delta\alpha_0$ in single-ion standards has been performed by displacing the ion from trap center with a dc electric field. The ion is then subjected to the rf fields of the trapping potential and the clock transition experiences time-dilation and scalar Stark shifts. This method was used to measure polarizabilities in $^{138}\mathrm{Ba}^+$ [23] and $^{171}\mathrm{Yb}^+$ [24] with uncertainties of 8% and 20%, respectively. A difficulty with this type of measurement is the evaluation of the electric field with high accuracy.

Our measurement method is based on the observation that the quadratic scalar Stark shift and the time-dilation shift caused by micromotion are correlated and have opposite signs for the $S-D$ transition of $^{88}\mathrm{Sr}^+$ [17]. This is only possible for transitions with $\Delta\alpha_0 < 0$, for example, the $^2S_{1/2} - {}^2D_{5/2}$ transitions of $^{40}\mathrm{Ca}^+$ [25], $^{43}\mathrm{Ca}^+$ [26], $^{88}\mathrm{Sr}^+$ [22], $^{138}\mathrm{Ba}^+$ [27], and $^{225}\mathrm{Ra}^+$ [27]. For this class of transitions, the trap drive frequency Ω_0 at which the two micromotion-related effects cancel each other is determined by $\Delta\alpha_0$. In first-order approximation, the relation is [17,28]

$$\Omega_0^2 \simeq -\frac{h\nu_0}{\Delta\alpha_0}\left(\frac{e}{mc}\right)^2, \quad (2)$$

where ν_0 is the clock frequency in Hz [5,29], e the elementary charge, and m the mass of $^{88}\mathrm{Sr}^+$. The method does not depend on the electric field strength. Here, with a measurement of Ω_0, we improve $\Delta\alpha_0$ by a factor of 24 compared to the best atomic structure calculations [22]. To our knowledge, the result reported here is currently the most accurate measurement of a differential static scalar polarizability of an ion clock transition.

Ω_0 was measured by comparing two $^{88}\mathrm{Sr}^+$ ion trap systems, one used as a reference and the other used as a test trap to study the change in micromotion shifts with trap frequency. The reference system is an ion trap of the end cap design with an evaluated uncertainty of 10 mHz or 2.3×10^{-17} in fractional frequency units [17]. It was operated with a constant rf frequency and under the same conditions as those of the evaluation in Ref. [17] to provide a very reproducible ion frequency reference for the comparison. Before each measurement run, the ion micromotion was minimized. As a result, the fractional time-dilation and Stark shifts, when considered separately, were $\lesssim 3.4(4) \times 10^{-17}$. These correlated shifts are reduced by a factor of 180 at the trap frequency of $\Omega/2\pi = 14.39$ MHz, yielding net micromotion shifts of 2×10^{-19}. An ion temperature of 1.5(5) mK was measured, in agreement with previous results [17].

The test system is a Paul-type quadrupole ion trap with a single optical access port [30]. It has uncompensated fractional micromotion shifts of $\approx 7 \times 10^{-14}$ that were used for the purpose of the present study. The shifts are attributed to ion displacement caused by stray electric fields from the electrode surfaces and residual trap imperfections. The micromotion shifts cannot be completely minimized because adjustment of the ion position is only possible along the trap z axis in the current design. Nevertheless, for optimum reproducibility of the ion position in the trap, micromotion was minimized along the cooling laser beam direction before each measurement. The ion temperature was 1.8(9) mK. The test trap was operated with frequencies between 13.5 and 15.0 MHz to cover the zero-crossing frequency of 14.39 (25) MHz predicted by theory [17]. The rf trap voltage amplitude V_0 was adjusted to maintain constant ion secular frequencies (trap restoring forces) throughout the measurements [31]. V_0 was measured with a 1% reproducibility using a high-voltage probe and an oscilloscope. The relation between V_0 and the secular frequencies was established with a measurement of the secular frequencies at a trap frequency of 14.429 MHz: $\omega_x/2\pi = 1.165(5)$ MHz, $\omega_y/2\pi = 1.193(5)$ MHz, and $\omega_z/2\pi = 2.419(5)$ MHz.

The two traps were operated from common solid-state laser sources: a 422 nm laser for cooling on the $^2S_{1/2} - {}^2P_{1/2}$ transition, a 1092 nm repumper laser to prevent decay from the $^2P_{1/2}$ state to the $^2D_{3/2}$ state, a 674 nm laser to probe the S–D clock transition [32], and a 1033 nm laser tuned to the $^2D_{5/2} - {}^2P_{3/2}$ transition to return the ion to the ground state before the start of each interrogation cycle. Independent acousto-optic modulators were used to frequency shift the 674 nm radiation into resonance with each ion. The difference between the acousto-optic modulator frequencies then gave the offset between the two ion trap systems. The laser pulses were synchronized, but the frequency locks to the clock transition line centers were independent. The line centers were measured using three pairs of symmetric Zeeman components to cancel the linear Zeeman, the electric quadrupole, and the tensor Stark shifts [17,33].

Figure 1 shows the comparison data of the two ion frequency standards as a function of the rf drive frequency of the test trap. The data were recorded over a six-week period in a random order. There is no indication of a change in stray electric fields during the experiments. The uncertainty assigned to each point in Fig. 1 has two components. The first is the measurement uncertainty given by the Allan deviation of the comparison data. The second is caused by the 1% uncertainty in setting the trap voltage V_0. Variations in V_0 modify the micromotion levels, thus causing an additional uncertainty in the frequency difference between the two ion standards.

To make an accurate measurement of Ω_0, the frequency offset between the two ions must be evaluated. The detailed analysis given in Ref. [17] is used for both systems. It applies without change to the reference trap except for a lower uncertainty on the BBR shift obtained with the measurement of $\Delta\alpha_0$ reported here. For the test trap, the net micromotion shift must be excluded from the evaluation as it is the effect being measured.

The dominant uncertainty in the evaluation of the frequency offset between the two ions is from the BBR shift. Other shifts are negligible in the current study compared to the trap comparison measurement uncertainty of 50 mHz.

The vacuum chamber temperatures were measured with calibrated thermistors during the experiments. The thermal

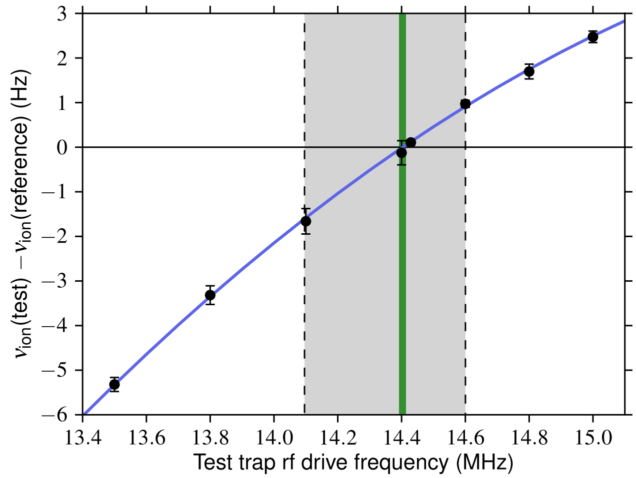

FIG. 1 (color online). Frequency difference between two ion standards as a function of the rf drive frequency of the trap with high micromotion levels (test trap). The curve is a fit to the data using the polynomial $a(f-f_0)^2+b(f-f_0)$ to determine the trap frequency $f_0=\Omega_0/2\pi$ and the slope b at the zero crossing. The fit gives $f_0=14.404(10)$ MHz and $b=4.86(13)$ Hz/MHz. f_0 is used to determine $\Delta\alpha_0$ and b the mean-squared electric field $\langle E^2\rangle$. The narrow vertical band and the shaded area delimited by dashed lines illustrate the uncertainty of, respectively, the current experimental work and a theoretical result [22]. The statistical uncertainty of the frequency comparison at the zero crossing is 50 mHz.

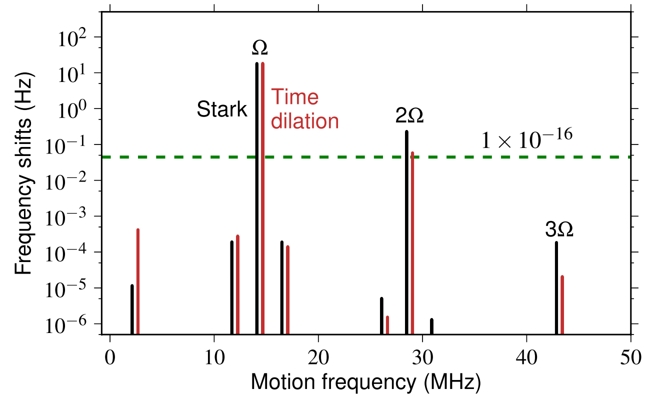

FIG. 2 (color online). Calculated spectrum of the driven and secular motion frequency shifts of the $^{88}Sr^+$ clock transition in the test trap. For clarity, only the axial secular motion is shown. The simulation parameters are $\Omega/2\pi=14.404$ MHz, $T_{ion}=1.8$ mK, $E_{rms}=9.84$ kV/m, and $\omega_z/2\pi=2.419$ MHz. The Stark and time-dilation spectra are intentionally split to show their relative contributions, with the positive Stark components shifted left and the negative time-dilation components shifted right. The dashed line shows the 50 mHz (1×10^{-16}) uncertainty level of the data.

model presented in Ref. [17] was used for the reference trap. For the test trap, the BBR field is determined by the vacuum chamber wall temperature, with a negligible contribution from electrode heating as a result of the small electrode capacitance and the trap construction. The uncertainty of this assumption is estimated to be 1.5 °C. The average frequency difference between the trapped ions caused by the BBR shift is $\Delta\nu_{BBR}(\text{test})-\Delta\nu_{BBR}(\text{reference})=5(7)$ mHz. Each point in Fig. 1 was corrected for the BBR shift difference evaluated during its measurement.

The data of Fig. 1 give $\Omega_0/2\pi=14.404(10)$ MHz. We need to consider the ion motion in the test trap in some detail to further determine $\Delta\alpha_0$ from Ω_0 with a higher accuracy than is possible from Eq. (2). Micromotion at the trap drive frequency Ω is the dominant component. There is also motion at the harmonics $n\Omega$ and thermal motion sidebands at the radial and axial secular frequencies. A calculated spectrum for the operating conditions of the test trap obtained by solving the equation of motion to high order is shown in Fig. 2 [34,35]. The important features for our analysis, caused by ion displacement, are at Ω and 2 Ω. The other features below the mHz level are negligible. Note that there is no dc Stark shift component because the stationary stray electric field is exactly canceled by the rf trap when the ion is at its equilibrium position (see the Supplemental Material [36]).

A general expression for the net micromotion shift $\Delta\nu_\mu$ is a sum over the trap drive harmonics of motion due to the scalar Stark shift and the time-dilation shift,

$$\Delta\nu_\mu=-\frac{\nu_0}{2}\sum_i\sum_{n=1}^{\infty}\left[\frac{\Delta\alpha_0}{h\nu_0}+\frac{1}{n^2}\left(\frac{e}{m\Omega c}\right)^2\right]\langle E_i^2(n\Omega)\rangle, \quad (3)$$

where i is a summation index over r and z, for, respectively, motion in the radial and axial directions in the trap. $\langle E_i^2(n\Omega)\rangle$ is the mean-squared electric field at the frequency $n\Omega$. The first term in square brackets is proportional to the scalar Stark shift and the second term is proportional to the time-dilation shift.

The $\langle E_i^2(n\Omega)\rangle$ field intensities are calculated by solving the equation of motion when a dc electric field displaces the ion from the center of the quadrupole potential. The second-order solution in Ω gives (see the Supplemental Material [36])

$$\rho_i\equiv\frac{\langle E_i^2(2\Omega)\rangle}{\langle E_i^2(\Omega)\rangle}=\left(\frac{4q_i}{a_i-16}\right)^2, \quad (4)$$

where a_i and q_i are the so-called Mathieu parameters. In an ideal quadrupole potential, they are given by $a_z=-2a_r=-16eU_0/m\Omega^2d^2$ and $q_z=-2q_r=8eV_0/m\Omega^2d^2$, where d is a characteristic length that depends on trap geometry [24,31,35]. U_0 is a static voltage applied between the ring and end cap electrodes.

Solving Eq. (3) to second order in Ω for $\Delta\nu_\mu=0$, we obtain

$$\Delta\alpha_0 = -\frac{h\nu_0}{\Omega_0^2}\left(\frac{e}{mc}\right)^2\left[\frac{(1+\rho_z/4)+\xi(1+\rho_r/4)}{(1+\rho_z)+\xi(1+\rho_r)}\right], \quad (5)$$

where $\xi \equiv \langle E_r^2(\Omega)\rangle/\langle E_z^2(\Omega)\rangle$. Equation (5) is accurate at the 30 ppm level compared to a higher-order solution. The term in square brackets indicates that the first-order result of Eq. (2) overestimates $\Delta\alpha_0$ by $\approx 0.6\%$ for our experimental conditions.

The test trap Mathieu parameters are required for ρ_r and ρ_z. The trap was operated with $U_0 = 0$, which gives $a_r = a_z = 0$. q_r and q_z were obtained from the secular frequencies. Applying a small correction due to the frequency response of the V_0 measurements, we obtain $q_r = (q_x + q_y)/2 = -0.2283(18)$ and $q_z = 0.4521(26)$ at 14.404 MHz. The uncertainties depend on contributions from the secular frequencies, the 1% reproducibility of V_0, and, for q_r, an additional uncertainty from the nondegeneracy of q_x and q_y. Using Eq. (4), we find $\rho_r = 0.003\,26(5)$ and $\rho_z = 0.012\,77(15)$.

The parameter ξ depends on the direction of the electric field. If β defines the angle between the trap z axis and the total electric field at the ion $\mathbf{E}(t) = E_r(t)\hat{\mathbf{r}} + E_z(t)\hat{\mathbf{z}}$, we have $\tan^2\beta = \langle E_r^2\rangle/\langle E_z^2\rangle$. Using Eq. (4), we get to second order

$$\xi = \left(\frac{1+\rho_z}{1+\rho_r}\right)\tan^2\beta. \quad (6)$$

The electric field direction was determined from a tensor Stark shift measurement made with the magnetic field aligned with the trap axis. In this case, β can be determined from the slope with respect to $m_{J'}^2$ of the tensor Stark shift [17]

$$\frac{\partial(\Delta\nu_{\mathrm{tensor}})}{\partial m_{J'}^2} = -\frac{3\alpha_2}{40h}(3\cos^2\beta - 1)\langle E^2\rangle, \quad (7)$$

where α_2 is the $^2D_{5/2}$ level tensor polarizability [22]. The variation with $m_{J'}^2$ is readily obtained with our method used to lock to the S–D line center since the frequencies of three pairs of Zeeman components connecting to different upper state magnetic sublevels $m_{J'}$ are measured [17,33]. $\langle E^2\rangle = \langle\mathbf{E}\cdot\mathbf{E}\rangle = [9.84(13)\ \mathrm{kV/m}]^2$ is obtained from the slope at the x intercept of the trap comparison data of Fig. 1. Taking into account the alignment uncertainty of the magnetic field with the trap axis, the tensor Stark shift measurement gave $\beta = 43(4)^\circ$ and $\xi = 0.88(24)$.

Using the measured values of Ω_0, ρ_r, ρ_z, and ξ in Eq. (5), we find $\Delta\alpha_0 = -4.7938(71)\times 10^{-40}\ \mathrm{J\,m^2/V^2}$. Table I gives the uncertainty budget of $\Delta\alpha_0$. Because of correlation effects, the uncertainty contributions of ρ_r and ρ_z are reported as a single value. The parameter labeled "Other" combines smaller contributions. The limiting factor in the determination of $\Delta\alpha_0$ is the uncertainty of Ω_0, which is caused primarily by the statistical uncertainty of the trap comparison measurements. The measurement of $\Delta\alpha_0$ reported here is in excellent agreement with the value $-4.83(17)\times 10^{-40}\ \mathrm{J\,m^2/V^2}$ obtained by atomic structure calculations [22].

TABLE I. $\Delta\alpha_0$ uncertainty budget.

Parameter	Value	$\Delta\alpha_0$ uncertainty ($10^{-43}\ \mathrm{J\,m^2/V^2}$)
Ω_0	14.404(10) MHz	6.65
ξ	0.88(24)	2.38
ΔBBR[a]	5(7) mHz	0.97
ρ_z	0.012 77(15)	0.34
ρ_r	0.003 26(5)	[b]
Other		0.18
Total		7.14

[a] $\Delta\mathrm{BBR} = \Delta\nu_{\mathrm{BBR}}(\mathrm{test}) - \Delta\nu_{\mathrm{BBR}}(\mathrm{reference})$.
[b] Contribution of ρ_r included with ρ_z.

Using the experimental value of $\Delta\alpha_0$ and the dynamic correction $\eta = -0.009\,51(15)$ in Eq. (1), we obtain a BBR shift coefficient of 0.247 99(37) Hz at 300 K. The contribution of the BBR coefficient to the $^{88}\mathrm{Sr}^+$ ion standard uncertainty has been reduced from a previously limiting value of 2×10^{-17} to 8.3×10^{-19}. An immediate benefit of the lower uncertainty is a reduction by a factor of 2 of the evaluation of the reference trap system to 1.2×10^{-17}, limited by the evaluation of the BBR field [17]. With a modest improvement to the BBR field temperature uncertainty of 1.5 °C, the total fractional uncertainty will reach into the 10^{-18} level. For example, an effective BBR temperature uncertainty of 0.2 °C would give a $^{88}\mathrm{Sr}^+$ ion uncertainty evaluation of 3×10^{-18}.

The work reported here provides a significant improvement in the BBR shift coefficient uncertainty of the $^{88}\mathrm{Sr}^+$ ion and allows for a reduction of the micromotion shifts in the reference trap by a factor of 200, down to the 10^{-19} level, by choosing the appropriate trap drive frequency. The electric quadrupole shift cancellation method, reported in previous work [17,33], allows a reduction of the electric quadrupole and tensor Stark shifts to the 10^{-19} level or lower. By combining the results reported here with the methods outlined in Refs. [17,33], the $^{88}\mathrm{Sr}^+$ ion standard has a clear potential for an extremely low and robust uncertainty evaluation.

In summary, we have reported a high-accuracy measurement of the differential static scalar polarizability $\Delta\alpha_0$ of the $5s\,^2S_{1/2} - 4d\,^2D_{5/2}$ transition of $^{88}\mathrm{Sr}^+$. The measurement method was based on the comparison of two ion standards, one in a reference trap and the other in a test trap with large micromotion shifts. At a special drive frequency Ω_0 of the test trap, the micromotion-induced scalar Stark and time-dilation shifts cancel each other. $\Delta\alpha_0$ was determined from Ω_0 using a second-order solution to include the effect of motion harmonics. The $\Delta\alpha_0$ fractional uncertainty obtained is 0.15%. Using $\Delta\alpha_0$ and the dynamic correction, the BBR shift coefficient was determined with an uncertainty of 0.37 mHz, giving a contribution of 8.3×10^{-19} to the evaluation of the $^{88}Sr^{+}$ ion standard at 300 K.

The authors thank M. S. Safronova for fruitful discussions regarding the dynamic correction coefficient, and W. Pakulski and B. Hoger for technical support.

*pierre.dube@nrc-cnrc.gc.ca

[1] C. W. Chou, D. B. Hume, J. C. J. Koelemeij, D. J. Wineland, and T. Rosenband, Phys. Rev. Lett. **104**, 070802 (2010).

[2] S. A. King, R. M. Godun, S. A. Webster, H. S. Margolis, L. A. M. Johnson, K. Szymaniec, P. E. G. Baird, and P. Gill, New J. Phys. **14**, 013045 (2012).

[3] N. Huntemann, M. Okhapkin, B. Lipphardt, S. Weyers, Chr. Tamm, and E. Peik, Phys. Rev. Lett. **108**, 090801 (2012).

[4] T. L. Nicholson, M. J. Martin, J. R. Williams, B. J. Bloom, M. Bishof, M. D. Swallows, S. L. Campbell, and J. Ye, Phys. Rev. Lett. **109**, 230801 (2012).

[5] A. A. Madej, P. Dubé, Z. Zhou, J. E. Bernard, and M. Gertsvolf, Phys. Rev. Lett. **109**, 203002 (2012).

[6] N. Hinkley, J. A. Sherman, N. B. Phillips, M. Schioppo, N. D. Lemke, K. Beloy, M. Pizzocaro, C. W. Oates, and A. D. Ludlow, Science **341**, 1215 (2013).

[7] R. Le Targat *et al.*, Nat. Commun. **4**, 3109 (2013).

[8] B. J. Bloom, T. L. Nicholson, J. R. Williams, S. L. Campbell, M. Bishof, X. Zhang, W. Zhang, S. L. Bromley, and J. Ye, Nature (London) **506**, 71 (2014).

[9] J. Guéna *et al.*, IEEE Trans. Ultrason. Ferroelectr. Freq. Control **59**, 391 (2012).

[10] A. Bauch, Meas. Sci. Technol. **14**, 1159 (2003).

[11] F. Riehle, *Frequency Standards* (Wiley-VCH, Berlin, 2004), and references therein.

[12] O. O. Versolato, L. W. Wansbeek, K. Jungmann, R. G. E. Timmermans, L. Willmann, and H. W. Wilschut, Phys. Rev. A **83**, 043829 (2011).

[13] M. N. Portela *et al.*, Appl. Phys. B **114**, 173 (2014).

[14] P. Gill and F. Riehle, in *Proceedings of the 2012 Conference on Precision Electromagnetic Measurements* (IEEE, New York, 2012), pp. 187–188.

[15] F. Riehle, Physics **5**, 126 (2012).

[16] M. S. Safronova, M. G. Kozlov, and C. W. Clark, Phys. Rev. Lett. **107**, 143006 (2011).

[17] P. Dubé, A. A. Madej, Z. Zhou, and J. E. Bernard, Phys. Rev. A **87**, 023806 (2013).

[18] J. A. Sherman, N. D. Lemke, N. Hinkley, M. Pizzocaro, R. W. Fox, A. D. Ludlow, and C. W. Oates, Phys. Rev. Lett. **108**, 153002 (2012).

[19] T. Middelmann, S. Falke, C. Lisdat, and U. Sterr, Phys. Rev. Lett. **109**, 263004 (2012).

[20] W. M. Itano, L. L. Lewis, and D. J. Wineland, Phys. Rev. A **25**, 1233 (1982).

[21] S. G. Porsev and A. Derevianko, Phys. Rev. A **74**, 020502 (2006).

[22] D. Jiang, B. Arora, M. S. Safronova, and C. W. Clark, J. Phys. B **42**, 154020 (2009).

[23] N. Yu, X. Zhao, H. Dehmelt, and W. Nagourney, Phys. Rev. A **50**, 2738 (1994).

[24] T. Schneider, E. Peik, and Chr. Tamm, Phys. Rev. Lett. **94**, 230801 (2005).

[25] M. S. Safronova and U. I. Safronova, Phys. Rev. A **83**, 012503 (2011).

[26] B. Arora, M. S. Safronova, and C. W. Clark, Phys. Rev. A **76**, 064501 (2007).

[27] B. K. Sahoo, R. G. E. Timmermans, B. P. Das, and D. Mukherjee, Phys. Rev. A **80**, 062506 (2009).

[28] D. J. Berkeland, J. D. Miller, J. C. Bergquist, W. M. Itano, and D. J. Wineland, J. Appl. Phys. **83**, 5025 (1998).

[29] H. S. Margolis, G. P. Barwood, G. Huang, H. A. Klein, S. N. Lea, K. Szymaniec, and P. Gill, Science **306**, 1355 (2004).

[30] A. A. Madej, J. E. Bernard, P. Dubé, L. Marmet, and R. S. Windeler, Phys. Rev. A **70**, 012507 (2004).

[31] D. J. Wineland, W. M. Itano, and R. S. Van Dyck, Jr., in *High-Resolution Spectroscopy of Stored Ions*, edited by D. Bates and B. Bederson, Advances in Atomic and Molecular Physics Vol. 19 (Academic Press, New York, 1983), pp. 135–186.

[32] P. Dubé, A. A. Madej, J. E. Bernard, L. Marmet, and A. D. Shiner, Appl. Phys. B **95**, 43 (2009).

[33] P. Dubé, A. A. Madej, J. E. Bernard, L. Marmet, J.-S. Boulanger, and S. Cundy, Phys. Rev. Lett. **95**, 033001 (2005).

[34] N. W. McLachlan, *Theory and Application of Mathieu Functions* (Clarendon Press, Oxford, 1947).

[35] R. F. Wuerker, H. Shelton, and R. V. Langmuir, J. Appl. Phys. **30**, 342 (1959).

[36] See Supplemental Material at http://link.aps.org/supplemental/10.1103/PhysRevLett.112.173002 for a derivation of the electric field for a single-ion in a rf quadrupole trap when there is a stationary stray electric field.